Research Article | Vol. 27, No. 15 | 22 Jul 2019 | OPTICS EXPRESS 20098
Optics EXPRESS

Determination of complex dielectric function of $CH_3NH_3PbBr_3$ perovskite cubic colloidal quantum dots by modified iterative matrix inversion method

HEE CHUL WOO,[1,4] JIN WOO CHOI,[2,4] JAE-SUK LEE,[3,5] AND CHANG-LYOUL LEE[1,6]

[1]*Advanced Photonics Research Institute (APRI), Gwangju Institute of Science and Technology (GIST), Gwangju 61005, South Korea*
[2]*Surface Technology Division, Korea Institute of Materials Science (KIMS), Changwon 51508, South Korea*
[3]*School of Material Science and Engineering, Gwangju Institute of Science and Technology (GIST), Gwangju 61005, South Korea*
[4]*These authors contributed equally to this work*
[5]*jslee@gist.ac.kr*
[6]*vsepr@gist.ac.kr*

Abstract: Recent advances in lead halide perovskite quantum dots appeal with their potential in various optoelectronic devices such as photovoltaics, photodetectors, light-emitting diodes (LEDs) and lasers. However, lack of information on the intrinsic optical properties of lead halide perovskite quantum dots (QDs) lags the progress in device performances and further development in various applications. In this letter, the complex dielectric function of $CH_3NH_3PbBr_3$ perovskite cubic colloidal QDs was determined from the UV-Vis absorption by using a modified iterative matrix inversion (IMI) method. The modified IMI method takes into account the dilute solution with cubic inclusions, while the conventional method only considers spherical or elliptical inclusions by Maxwell-Garnett (MG) effective medium theory. In addition, singly subtractive Kramer Kronig (SSKK) relations have also been considered to compensate for possible errors arising from the finite wavelength range of the experimental absorption data.

1. Introduction

The accurate optical constants of semiconducting materials are essential for designing optoelectronic devices, such as photovoltaic, photodetector, light emitting diodes (LEDs) and lasers. For example, the complex dielectric function, $\boldsymbol{\varepsilon} = \varepsilon_R + i\varepsilon_I$ and the complex refractive index, $\mathbf{n} = n + i\kappa$ have already been widely used to determine the quantum confinement effect [1–3] and to estimate external quantum efficiency of LEDs [4–6]. Recently, perovskite quantum dots (QDs) have emerged as a potential candidate for various optoelectronic devices due to their excellent optical and electrical properties, such as high photoluminescence quantum yield (PLQY), high exciton binding energy and decent electrical conductivity, etcs [7–9]. In spite of their great experimental optoelectronic properties, however, quite limited information on the intrinsic optical constants of perovskite QDs is reported. Some recent reports on the optical constants of lead halide perovskites are for thin film and single crystal but not for QDs [10–14]. Moreover, those are mostly based on spectroscopic ellipsometry that usually requires pinhole-free and optically smooth surface samples on the standard glass or silicon substrates.

In general, the data analysis of the spectroscopic ellipsometry requires an optical model defined by various sample conditions, such as chemical composition, grain size, crystallinity

#362362 https://doi.org/10.1364/OE.27.020098
Journal © 2019 Received 13 Mar 2019; revised 23 Jun 2019; accepted 24 Jun 2019; published 8 Jul 2019

Optics EXPRESS

and thickness [15,16]. This implies that the material properties acquired from the spectroscopic ellipsometry are largely dependent on the extrinsic factors. Therefore, the spectroscopic ellipsometry is not the appropriate characterization method for obtaining intrinsic optical constant of colloidal QDs (CQDs). One simple method for obtaining intrinsic optical constants of CQDs is to extract the intrinsic optical properties from the absorption spectrum [17]. The main idea of this method is to compare the experimental absorption spectrum with the theoretical absorption spectrum derived from dielectric function of the colloidal QDs.

In this study, the complex dielectric function of $CH_3NH_3PbBr_3$ perovskite cubic colloidal QDs was determined from the UV-Vis absorption by using modified iterative matrix inversion (IMI) method. The modified IMI method takes into account the dilute solution with cubic inclusions, while the conventional method only considers spherical or elliptical inclusions by Maxwell-Garnett (MG) effective medium theory. In addition, singly subtractive Kramer Kronig (SSKK) relations have also been considered to compensate possible errors arising from the finite wavelength range of the experimental absorption data.

2. Sample preparation and methods

The $CH_3NH_3PbBr_3$ CQDs were synthesized by the precipitation method. To prepare precursor solution, 0.4mmol of $PbBr_2$ and 0.3 mmol of methylammonium bromide (CH_3NH_3Br) were mixed with 100 μL of OAm and 1 mL of OAc in 10 mL of dimethylformamide (DMF) solvent. 0.5 mL of precursor solution was then injected into 5 mL of benzene for the precipitation of $CH_3NH_3PbBr_3$ nanocrystals. After the injection, the precipitates of $CH_3NH_3PbBr_3$ nanocrystals are formed, and the transparent solution turned into bright green or blue immediately depending on their shape and size. Synthesized nanocrystals were then further purified to obtain $CH_3NH_3PbBr_3$ QDs with target diameters and shape.

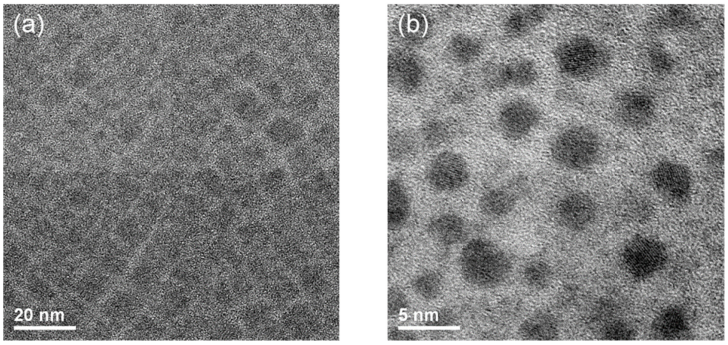

Fig. 1. TEM image of synthesized (a) cubic and (b) spherical $CH_3NH_3PbBr_3$ CQDs.

In order to control the size and shape of QDs, the temperature of the benzene was controlled before the injection of precursor solution. Figure 1 shows the TEM image of synthesized cubic and spherical CQDs with different injection temperature, 40 and 25℃ respectively. The cubic QDs were obtained at 40℃ while the spherical QDs were obtained at 25℃.

3. Results and Discussion

The main idea of this method is to compare the experimental absorption spectrum with the theoretical absorption spectrum derived from dielectric function of the colloidal QDs. The derivation of the theoretical absorption coefficient of colloidal QDs starts from the basic Lorentz-Lorenz model, which relates the effective dielectric function, ε_{eff} of CQD solution to the polarizability, α_n of QDs [18]:

Optics EXPRESS

$$\boldsymbol{\varepsilon}_{\mathbf{eff}} = \varepsilon_{sol} + \nu_n \boldsymbol{\alpha}_{\mathbf{n}} \tag{1}$$

where ε_{sol} is the real part of the solvent dielectric function and ν_f is the volume fraction of QDs in the solution. For the dilute solution, its absorption is mostly due to the imaginary part of the dielectric function, or $\mathrm{Im}[\boldsymbol{\varepsilon}_{\mathbf{eff}}]$ which can be approximated as $\mathrm{Im}[\boldsymbol{\varepsilon}_{\mathbf{eff}}] \simeq \mathrm{Im}[\boldsymbol{\alpha}_{\mathbf{n}}]$. The polarizability of spherical QDs in normalized form is

$$\boldsymbol{\alpha}_{\mathbf{n}} = 3\varepsilon_{sol} \frac{\boldsymbol{\varepsilon}_{\mathbf{r}} - \varepsilon_{sol}}{\boldsymbol{\varepsilon}_{\mathbf{r}} + 2\varepsilon_{sol}} \tag{2}$$

where $\boldsymbol{\varepsilon}_{\mathbf{r}} = \varepsilon_R + i\varepsilon_I$ is the relative dielectric function of spherical QDs. Therefore, the imaginary part of the dielectric function, $\mathrm{Im}[\boldsymbol{\varepsilon}_{\mathbf{eff}}]$ can be expressed as

$$\mathrm{I}\,\mathrm{Im}[\boldsymbol{\varepsilon}_{\mathbf{eff}}] \simeq \mathrm{Im}[\boldsymbol{\alpha}_{\mathbf{n}}] = \nu_f \frac{9\varepsilon_{sol}^2}{(\varepsilon_R + 2\varepsilon_{sol})^2 + \varepsilon_I^2} \varepsilon_I \tag{3}$$

Then the intrinsic effective absorption coefficient, μ_i of the dilute $(\nu_f < 1)$ QDs solution can be related to the intrinsic dielectric function in analytical form as

$$\mu_i = \frac{\mu}{\nu_f} = \left(\frac{9n_s^4}{(\varepsilon_R + 2n_s^2)^2 + \varepsilon_I^2} \right) = \frac{2\pi\varepsilon_I}{\lambda n_s} \left| f_{sq} \right|^2 \tag{4}$$

which is also known as Maxwell-Garnett (MG) effective medium theory, where $n_s = \sqrt{\varepsilon_{sol}}$ is the real refractive index of the solvent and f_{sq} represents local field factor for dielectric sphere [19]. Meanwhile, the absorption coefficient can also be determined from experimental absorbance, A by

$$\mu_i = \frac{\mu}{\nu_f} = \frac{A \ln 10}{\nu_f L} \tag{5}$$

where μ and L are the experimental absorption coefficient and the optical path length, respectively.

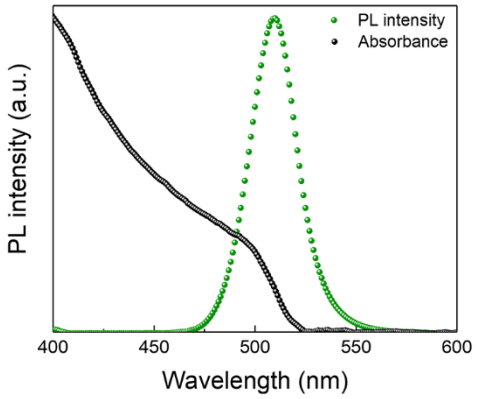

Fig. 2. Photoluminescence and absorption of $CH_3NH_3PbBr_3$ perovskite cubic CQDs.

As mentioned earlier, the idea is to repeat calculation of the theoretical absorption spectrum by varying dielectric function, until it becomes identical to the experimental values. The dielectric function is determined when the theoretical values converge to the

experimental values, and this is known as iterative matrix inversion (IMI) method. However, the conventional IMI method is valid only for spherical QDs which are not always true for the actual QDs that can be in any shape, such as polyhedrons, circular cylinder, ellipsoid, including spheres as well. For example, in our case, the optimized green emitting (510 nm) perovskite QDs are synthesized as ~10 nm cubic particles (Fig. 1(a) and Fig. 2) while the same synthesis with lower temperature gives spherical QDs (Fig. 1(b)). Therefore, the conventional method needs further modification for evaluating more accurate optical constants of cubic QDs.

Researchers have already reported the accurate estimate for the normalized polarizability of a dielectric cube [18,20]

$$\boldsymbol{\alpha}_{\mathbf{n}} = \frac{\alpha_{\infty}(\boldsymbol{\varepsilon}_{\mathbf{r}} - 1)(\boldsymbol{\varepsilon}_{\mathbf{r}}^{3} + 4.83981\boldsymbol{\varepsilon}_{\mathbf{r}}^{2} + 5.54742\boldsymbol{\varepsilon}_{\mathbf{r}} - \alpha_{0})}{\boldsymbol{\varepsilon}_{\mathbf{r}}^{4} + 8.0341\boldsymbol{\varepsilon}_{\mathbf{r}}^{3} + 19.3534\boldsymbol{\varepsilon}_{\mathbf{r}}^{2} + 15.4349\boldsymbol{\varepsilon}_{\mathbf{r}} + \alpha_{\infty}} \tag{6}$$

where $\boldsymbol{\varepsilon}_{\mathbf{r}}$ is the relative dielectric function of the cubic QDs, α_{∞} is 36.442 for a conducting cube and α_0 is -1.6383 for an insulating cube. However, as the equation manifests, the polarizability of dielectric cube is expressed in numerical form. Therefore, it is very difficult to make analytic relation between μ_i and $\boldsymbol{\varepsilon}_{\mathbf{r}}$ for the mixture of solution with cubic inclusions.

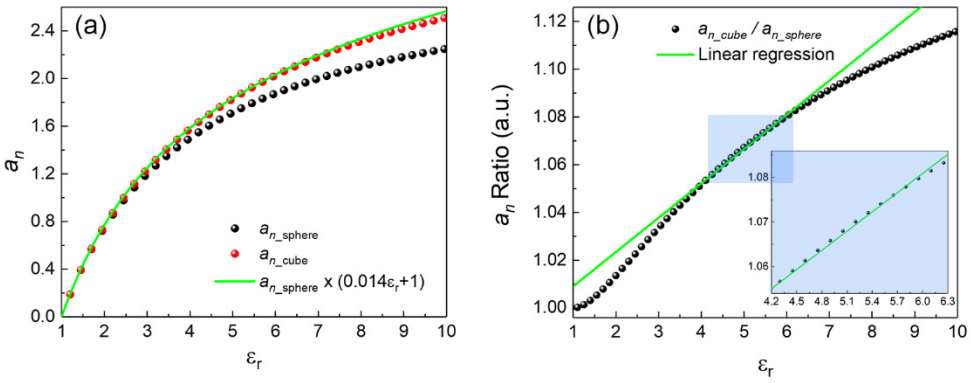

Fig. 3. (a) The polarizability of dielectric sphere and cube. (b) The polarizability ratio of dielectric cube to sphere as a function of ε_r (inset: magnified for actual ε_r range).

Figure 3(a) shows the polarizability, $\boldsymbol{\alpha}_{\mathbf{n}}$ of dielectric sphere and cube calculated using Eqs. (2) and (6) with $\boldsymbol{\varepsilon}_{\mathbf{r}} > 1$. It is observed that the polarizability of a dielectric cube is always larger than that of sphere. This implies that the dielectric cube shows stronger response to an external field than the sphere. Hence, it is also assumed that the local field factor of dielectric cube must be stronger than that of sphere, which will later be discussed. Figure 3(b) represents the polarizability ratio of dielectric cube to sphere $(\boldsymbol{\alpha}_{\mathbf{ncube}} / \boldsymbol{\alpha}_{\mathbf{nsphere}})$ as a function of $\boldsymbol{\varepsilon}_{\mathbf{r}}$. To simplify the polarizability of cube in analytical form, $\boldsymbol{\alpha}_{\mathbf{ncube}} / \boldsymbol{\alpha}_{\mathbf{nsphere}}$ was approximated by following first order linear equation:

$$\boldsymbol{\alpha}_{\mathbf{ncube}} / \boldsymbol{\alpha}_{\mathbf{nsphere}} \simeq 0.014\boldsymbol{\varepsilon}_{\mathbf{r}} + 1 \tag{7}$$

in $4.3 \le \boldsymbol{\varepsilon}_{\mathbf{r}} \le 6.3$ where the actual $\boldsymbol{\varepsilon}_{\mathbf{r}}$ of bulk $CH_3NH_3PbBr_3$ perovskite varies in the visible wavelength region [10]. Therefore, the polarizability of cube can now be written in simple analytical form as

Optics EXPRESS

$$\begin{aligned}\boldsymbol{\alpha}_{\mathbf{ncube}} &= \boldsymbol{\alpha}_{\mathbf{nsphere}} \times (0.014\boldsymbol{\varepsilon}_{\mathbf{r}} + 1) \\ &= 3\varepsilon_{sol} \frac{\boldsymbol{\varepsilon}_{\mathbf{r}} - \varepsilon_{sol}}{\boldsymbol{\varepsilon}_{\mathbf{r}} + 2\varepsilon_{sol}} (0.014\boldsymbol{\varepsilon}_{\mathbf{r}} + 1)\end{aligned} \tag{8}$$

The calculated polarizability of dielectric cube using Eq. (8) is plotted as a solid line in Fig. 2(a), which is almost the same as polarizability calculated by numerical form, Eq. (7). Then the imaginary part, $\mathrm{Im}[\boldsymbol{\alpha}_{\mathbf{ncube}}]$ can be expressed as

$$\mathrm{Im}[\boldsymbol{\alpha}_{\mathbf{ncube}}] = \left(0.042\varepsilon_{sol} + \frac{9\varepsilon_{sol}^2 (1 - 0.028\varepsilon_{sol})}{(\varepsilon_R + 2\varepsilon_{sol})^2 + \varepsilon_I^2} \right) \varepsilon_I \tag{9}$$

The intrinsic effective absorption coefficient of the cubic QD solution, ρ_i is

$$\rho_i = \frac{2\pi\varepsilon_I}{\lambda n_s} \left(0.042\varepsilon_{sol} + \frac{9\varepsilon_{sol}^2 (1 - 0.028\varepsilon_{sol})}{(\varepsilon_R + 2\varepsilon_{sol})^2 + \varepsilon_I^2} \right) = \frac{2\pi\varepsilon_I}{\lambda n_s} \left| f_{cq} \right|^2 \tag{10}$$

where f_{cq} represents the local field factor for dielectric cube. This can be rewritten in terms of effective absorption coefficient of the spherical QD solution, μ_i

$$\rho_i = \frac{2\pi}{\lambda n_s} (0.042\varepsilon_{sol}) + (1 - 0.028\varepsilon_{sol}) \mu_i \tag{11}$$

The analytical form of theoretical absorption coefficient for dielectric sphere and cube is now defined as μ_i and ρ_i, respectively. For its later use in the modified IMI method, ρ_i can be re-arranged as

$$\mu_i = \frac{\rho_i - \frac{2\pi}{\lambda n_s} (0.042\varepsilon_{sol}) \varepsilon_I}{(1 - 0.028\varepsilon_{sol})} \tag{12}$$

The modified IMI method considers singly subtractive Kramer-Kronig (SSKK) relation to estimate more accurate dielectric function from experimental absorption spectrum. The conventional KK relation requires the input ε_I values in infinite spectral range to obtain exact ε_R which is not possible in actual experimental conditions. Bachrach and Brown firstly introduced SSKK relation [21] in order to reduce the errors caused by the finite spectrum as they calculated the real refractive index of a medium from a measured absorption spectrum. The modified IMI method starts with SSKK relations in the discrete frequency form

$$\varepsilon_R(\omega_j) - \varepsilon_R(\omega_1) = \frac{2}{\pi} \sum_{k \neq j} \frac{(\omega_j^2 - \omega_1^2) \omega_k \Delta\omega}{(\omega_k^2 - \omega_j^2)(\omega_k^2 - \omega_1^2)} \varepsilon_I(\omega_k) \tag{13}$$

where ω_1 is the reference frequency at which we already know the value of $\varepsilon_R(\omega_1)$. As we take ε_I and ε_R as column vectors, the equation can be written in matrix form:

$$\varepsilon_R = \varepsilon_R(\omega_1) + \frac{2}{\pi} \mathbf{A} \cdot \Delta\varepsilon_I \tag{14}$$

with

Optics EXPRESS

$$\mathbf{A}_{j,k} = \frac{(\omega_j^2 - \omega_1^2)\omega_k \Delta\omega}{(\omega_k^2 - \omega_j^2)(\omega_k^2 - \omega_1^2)}, \mathbf{A}_{j,j} = 0 \tag{15}$$

Then the changes in real and imaginary parts of the dielectric function can also be expressed as

$$\Delta\varepsilon_R = \frac{2}{\pi}\mathbf{A} \cdot \Delta\varepsilon_I \tag{16}$$

The difference between experimental and theoretical values of $\Delta\mu_i$ can be expressed in terms of ε_I and ε_R by taking the first-order Taylor expansion:

$$\Delta\mu_i = \Delta\varepsilon_I \left.\frac{\partial\mu_i}{\partial\varepsilon_R}\right|_{\varepsilon_0} + \Delta\varepsilon_I \left.\frac{\partial\mu_i}{\partial\varepsilon_I}\right|_{\varepsilon_0} \tag{17}$$

The substitution of $\Delta\varepsilon_R$ to $\Delta\varepsilon_I$ and the rearrangement of Eq. (17) gives,

$$\Delta\varepsilon_I = \left(\mathbf{C} + \frac{2}{\pi}\mathbf{D} \cdot \mathbf{A}\right)^{-1} \frac{\Delta\mu}{\mu_0} \tag{18}$$

where C and D are diagonal matrices with elements

$$\begin{aligned} \mathbf{C}_{j,j} &= \left(\frac{1}{\varepsilon_{I,0}} - \frac{2\varepsilon_{I,0}}{(\varepsilon_{R,0} + 2n_s^2)^2 + \varepsilon_{I,0}^2}\right), \mathbf{C}_{j,k} = 0 \\ \mathbf{D}_{j,j} &= -\frac{2(\varepsilon_{R,0} + 2n_s^2)}{(\varepsilon_{R,0} + 2n_s^2)^2 + \varepsilon_{I,0}^2}, \mathbf{D}_{j,k} = 0 \end{aligned} \tag{19}$$

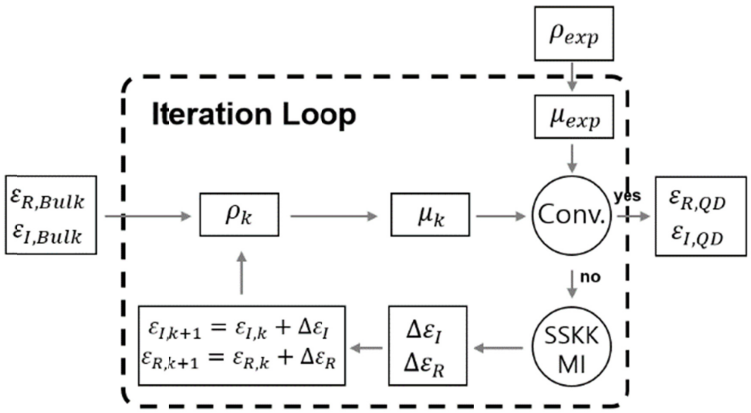

Fig. 4. Schematic representation of the modified iterative matrix inversion method. MG: Maxwell-Garnett, SSKK: singly subtractive Kramers-Kronig, MI: Matrix inversion.

Figure 4 shows the scheme of our SSKK modified IMI method. It starts with trial ε_I and ε_R as input parameters and we put bulk ε_I and ε_R values of $CH_3NH_3PbBr_3$ single crystal measured by ellipsometry [10]. Then the theoretical absorption spectrum, ρ_i is directly calculated via Eq. (11). Both theoretical and experimental ρ_i values are converted to μ_i by Eq. (12) of which the difference is related with $\Delta\varepsilon_I$ by Eq. (18). The iterative calculation of

Optics EXPRESS

theoretical μ_i continues until it converges to experimental value and the input ε_R and ε_I are renewed as $\varepsilon_R + \Delta\varepsilon_R$ and $\varepsilon_I + \Delta\varepsilon_I$ for each calculation. Once the theoretical μ_i converges to experimental μ_i, with root-mean-square error below 10^{-6}, iteration stops and ε_I and ε_R are printed.

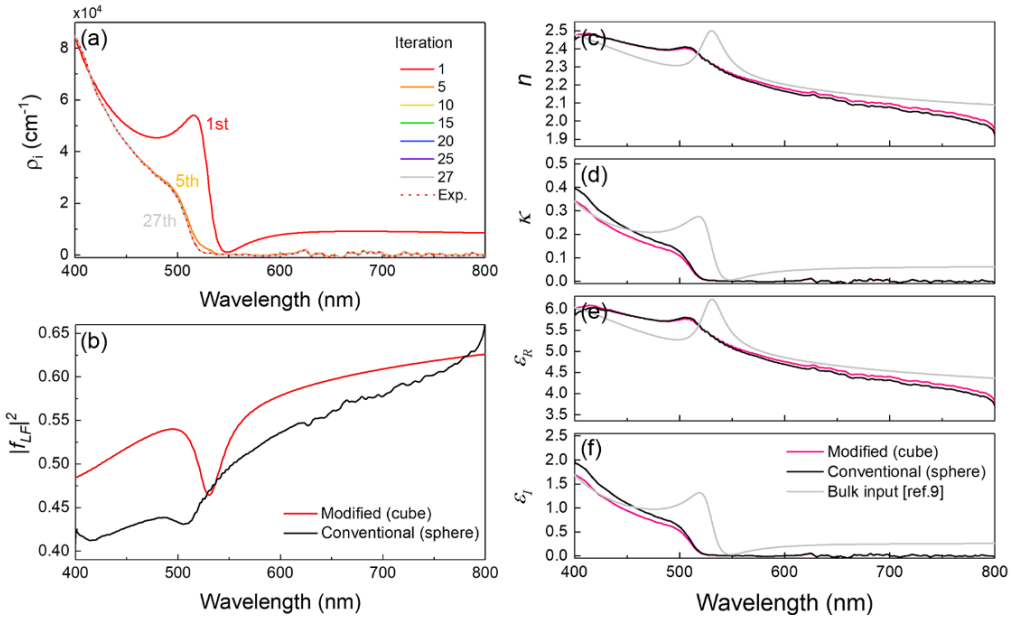

Fig. 5. The convergence of theoretical ρ_i to the experimental ρ_i. (b) The local field factors. The comparison of resultant (c,d) complex refractive index and (e,f) complex dielectric function.

Figure 5(a) shows the changes in ρ_i with modified IMI method. During each iteration, μ_i is recalculated and ρ_i is also updated. The theoretical ρ_i rapidly becomes close to the experimental ρ_i in only 5 iterations and it completely converges to the experimental ρ_i after 27 iterations.

The results obtained by both conventional and modified IMI methods for our $CH_3NH_3PbBr_3$ perovskite cubic CQDs are also compared. The conventional IMI method assumes our QDs be sphere, while the modified IMI assumes them to be cube. It is expected that cubic CQDs have larger local field factor than spherical CQDs because of their higher polarizability. Figure 5(b) represents the square of local field factors, $\left|f_{sq}\right|^2$ and $\left|f_{cq}\right|^2$ calculated by conventional and modified IMI method, respectively. As expected, $\left|f_{cq}\right|^2$ is larger than $\left|f_{sq}\right|^2$ in most of wavelength range where the QDs absorb light. The stronger local field of dielectric cube implies that it interacts more strongly with external field. This makes dielectric cube absorb and retard more light than sphere when they have the same optical constants. However, our calculation is based on the same experimental absorption spectrum, which assumes that the dielectric cube and sphere had absorbed the same amount of the light. Therefore, the conventional IMI method should show overestimated κ and ε_I for dielectric sphere. The results are represented in Figs. 5(c)-5(f). The real and imaginary part of the complex refractive index are represented in Figs. 5(c) and 5(d), and the real and imaginary part of the complex dielectric function are plotted in Figs. 5(e) and 5(f). As expected, the κ

Optics EXPRESS

and ε_1 values for dielectric sphere are observed to be larger than those for cube. These results show that the modified IMI method reflects well the shape-dependent changes in dielectric function for cubic QDs compared to spherical QDs.

4. Conclusion

In summary, we have extracted the intrinsic optical constants of $CH_3NH_3PbBr_3$ perovskite cubic CQDs directly from their absorption spectrum by using modified IMI method. The modified IMI method takes into account the dilute solution with dielectric cubes, while the conventional method only considers spherical or elliptical inclusions by MG effective medium theory. In addition, SSKK relations have also been considered to compensate possible errors arising from the finite wavelength range of the experimental absorption data. The developed method is applicable to analysis of various cubic colloidal QDs and understanding their fundamental properties.

Funding

National Research Foundation of Korea (NRF-2016R1A2B4013003 and NRF-2018R1A2A3075144); Research Fund of 2019 Gwangju Institute of Science and Technology (Research on Advanced Optical Science and Technology).

References

1. C.-W. Chen, S.-Y. Hsiao, C.-Y. Chen, H.-W. Kang, Z.-Y. Huang, and H.-W. Lin, "Optical properties of organometal halide perovskite thin films and general device structure design rules for perovskite single and tandem solar cells," J. Mater. Chem. A Mater. Energy Sustain. **3**(17), 9152–9159 (2015).
2. T. Chen, Y. Liu, M. Tse, O. Tan, P. Ho, K. Liu, D. Gui, and A. Tan, "Dielectric functions of Si nanocrystals embedded in a SiO_2 matrix," Phys. Rev. B Condens. Matter Mater. Phys. **68**(15), 153301 (2003).
3. X. Zhao, C. M. Wei, L. Yang, and M. Y. Chou, "Quantum confinement and electronic properties of silicon nanowires," Phys. Rev. Lett. **92**(23), 236805 (2004).
4. S. Moller and S. Forrest, "Improved light out-coupling in organic light emitting diodes employing ordered microlens arrays," J. Appl. Phys. **91**(5), 3324–3327 (2002).
5. Y. Sun and S. Forrest, "Enhanced light out-coupling of organic light-emitting devices using embedded low-index grids," Nat. Photonics **2**(8), 483–487 (2008).
6. M.-H. Park, J. Park, J. Lee, H. S. So, H. Kim, S.-H. Jeong, T.-H. Han, C. Wolf, H. Lee, S. Yoo, and T.-W. Lee, "Efficient perovskite light-emitting diodes using polycrystalline core-shell-mimicked nanograins," Adv. Funct. Mater. **29**(22), 1902017 (2019).
7. J. Woo Choi, H. C. Woo, X. Huang, W.-G. Jung, B.-J. Kim, S. W. Jeon, S. Y. Yim, J. S. Lee, and C. L. Lee, "Organic-inorganic hybrid perovskite quantum dots with high PLQY and enhanced carrier mobility through crystallinity control by solvent engineering and solid-state ligand exchange," Nanoscale **10**(28), 13356–13367 (2018).
8. H. C. Woo, J. W. Choi, J. Shin, S.-H. Chin, M. H. Ann, and C.-L. Lee, "Temperature-dependent photoluminescence of $CH_3NH_3PbBr_3$ perovskite quantum dots and bulk counterparts," J. Phys. Chem. Lett. **9**(14), 4066–4074 (2018).
9. L. Protesescu, S. Yakunin, M. I. Bodnarchuk, F. Krieg, R. Caputo, C. H. Hendon, R. X. Yang, A. Walsh, and M. V. Kovalenko, "Nanocrystals of cesium lead halide perovskite ($CsPbX_3$, X = Cl, Br, and I): novel optoelectronic materials showing bright emission with wide color gamut," Nano Lett. **15**(6), 3692–3696 (2015).
10. A. M. A. Leguy, P. Azarhoosh, M. I. Alonso, M. Campoy-Quiles, O. J. Weber, J. Yao, D. Bryant, M. T. Weller, J. Nelson, A. Walsh, M. van Schilfgaarde, and P. R. F. Barnes, "Experimental and theoretical optical properties of methylammonium lead halide perovskites," Nanoscale **8**(12), 6317–6327 (2016).
11. S. Brittman and E. C. Garnett, "Measuring *n* and *k* at the microscale in single crystals of $CH_3NH_3PbBr_3$ perovskite," J. Phys. Chem. C **120**(1), 616–620 (2016).
12. J.-S. Park, S. Choi, Y. Yan, Y. Yang, J. M. Luther, S.-H. Wei, P. Parilla, and K. Zhu, "Electronic structure and optical properties of α–$CH_3NH_3PbBr_3$ perovskite single crystal," J. Phys. Chem. Lett. **6**(21), 4304–4308 (2015).
13. P. Löper, M. Stuckelberger, B. Niesen, J. Werner, M. Filipič, S.-J. Moon, J.-H. Yum, M. Topič, S. De Wolf, and C. Ballif, "Complex refractive index spectra of $CH_3NH_3PbBr_3$ perovskite thin film determined by spectroscopic ellipsometry and spectrophotometry," J. Phys. Chem. Lett. **6**(1), 66–71 (2015).
14. M. Zhao, Y. Shi, J. Dai, and J. Lian, "Ellipsometric study of the complex optical constants of a $CsPbBr_3$ perovskite thin film," J. Mater. Chem. C Mater. Opt. Electron. Devices **6**(39), 10450–10455 (2018).
15. R. A. Synowicki, "Spectroscopic ellispometry characterization of indium tin oxide film microstructure and optical constants," Thin Solid Films **313**(314), 394–397 (1998).
16. Y. Jiang, A. M. Soufiani, A. Gentle, F. Huang, A. Ho-Baillie, and M. A. Green, "Temperature dependent optical properties of $CH_3NH_3PbBr_3$ perovskite by spectroscopic ellipsometry," Appl. Phys. Lett. **108**(6), 061905 (2016).

Optics EXPRESS

17. I. Moreels, G. Allan, B. D. Geyter, L. Wirtz, C. Delerue, and Z. Hens, "Dielectric function of colloidal lead chalcogenide quantum dots obtained by a Kramers-Kronig analysis of the absorbance spectrum," Phys. Rev. B Condens. Matter Mater. Phys. **81**(23), 235319 (2010).
18. A. Sihvola, J. Venermo, and P. Yla-Oijala, "Dielectric response of matter with cubic, circular-cylindrical, and spherical microstructure," Microw. Opt. Technol. Lett. **41**(4), 245–248 (2004).
19. Z. Hens and I. Moreels, "Light absorption by colloidal semiconductor quantum dots," J. Mater. Chem. **22**(21), 10406–10415 (2012).
20. A. Sihvola, "Dielectric polarization and particle shape effects," J. Nanomater. **2007**, 45090 (2007).
21. R. Z. Bachrach and F. C. Brown, "Exciton-optical properties of T1Br and T1C1," Phys. Rev. B **1**(2), 818–831 (1970).